Additional Supporting Documentation –
system parameters and compound files

A. Supporting documentation in the form of references has been provided to show how populations files are put together:

1. Howgate et al., 2006
2. Barter et al. 2013
3. V18R1 North European Caucasian population summary
4. V20R1 North European Caucasian population summary

In the former, key equations relating to the derivation of system specific parameters including demographics and cardiac output are described. In the second publication, the process itself is described.

In the third and fourth references above, the values and the source of input values relating to system parameters are cited.

Of note, for blood flows, a percentage of the cardiac output (CO) is apportioned to each tissue/organ flow (population summaries). For each virtual individual, a CO output based on body surface area (Howgate et al., 2006) is estimated; then the percentage CO values are used to calculate the flow rates into each organ/tissue.

There is population summary for V19R1 because there are few changes between the 2 versions.

B. Supporting documentation describing the development of some of the key compound files has also been provided in the form of publications:

5. Burt et al., 2016
6. Rowland Yeo et al., 2010
7. Rowland Yeo et al., 2011

In the above publications the development of key compound files is described, including cimetidine, verapamil, diltiazem and clarithromycin.

Although developed in earlier versions the parameters are the same as those used in V19.

In addition, in the second publication, we show the equations used to derive the competitive and mechanism-based inhibition of the perpetrators. Furthermore, in the third publication, we demonstrate why the kdeg value for CYP3A4 was updated.

Below, we describe the scaling approach and an overview of the PBPK models.

Scaling Methods and PBPK Models

Physiologically based pharmacokinetic models

A minimal physiologically based pharmacokinetic (PBPK) model, which considers both liver and intestinal metabolism (Figure A), is incorporated in the Simcyp Simulator. It includes a single adjusting compartment (SAC) that lumps all tissues excluding the intestine, liver and portal vein and can be used to represent those organs that make a significant contribution to the volume of distribution. The model can also be expanded to a full PBPK model by inclusion of additional tissues such as adipose, brain, bone, heart, lung, muscle and skin (Figure A2).

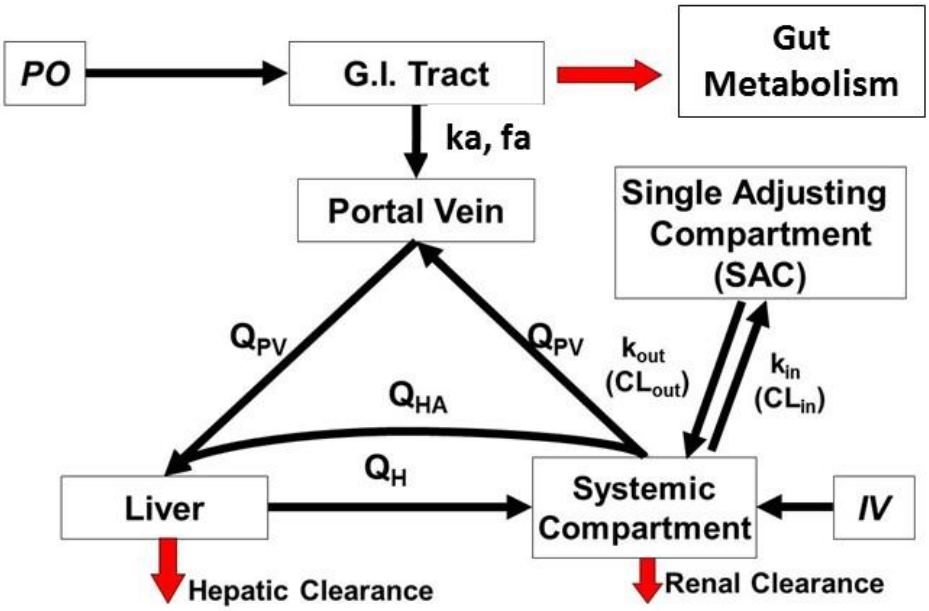

Figure A1. Minimal physiologically based pharmacokinetic model with single adjusting compartment. Q_H, Q_{PV}, and Q_{HA} are blood flows in the liver, portal vein, and hepatic artery, respectively; k_{in} and k_{out} are first order rate constants which act on the masses of drug within the systemic compartment and the SAC respectively; IV and PO are intravenous and oral dosing routes respectively; fa and ka are the fraction absorbed and the first order absorption rate constant, respectively.

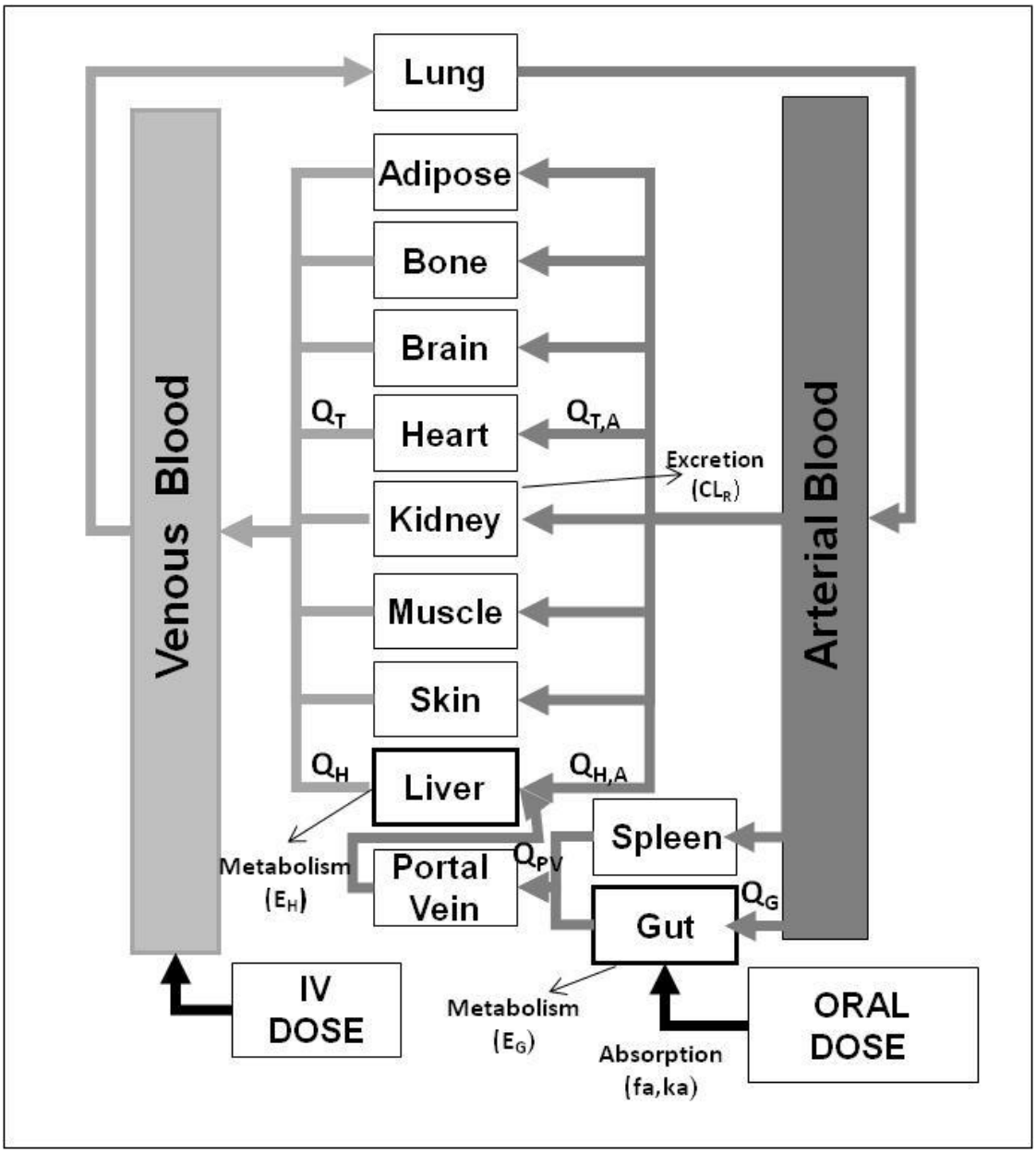

Figure A2. A physiologically based pharmacokinetic model. Q_H, $Q_{H,A}$, Q_{PV}, Q_G, $Q_{T,A}$ and Q_T are blood flows in the hepatic vein, hepatic artery, hepatic portal vein, gut and blood flows into and out of the other tissue (T) compartments, respectively; E_G and E_H are the fractions undergoing first pass metabolism in the gut and liver, respectively; CL_R is the renal clearance; fa and ka are the fraction absorbed and the first order absorption rate constant, respectively.

Prediction of V_{ss}

For the minimal model, an *in vivo* V_{ss} value (and associated variability) can be used as an input or this parameter can be predicted using Equation 1 from Sawada *et al*. (1984):

$$V_{ss} = (\sum V_t \times P_{t:p}) + (V_e \times E:P) + V_p$$

(Equation 1)

Where V is the fractional body volume (L/kg) of a tissue (t), erythrocyte (e), and plasma (p), E:P is the erythrocyte:plasma ratio and $P_{t:p}$ is the partition coefficient for non-adipose and adipose components. Three methods are available for prediction of $P_{t:p}$, the first reported by Poulin and Theil (2002) and modified by Berezhkovskiy (2004) and the second by Rodgers and Rowland (2006). The third method extends the Rodgers and Rowland method to account for the impact of membrane potential on the permeation of ionised drugs using the Fick-Nernst-Planck equation (Gaohua *et al.*, 2016).

Absorption Models

Several absorption models are available within the Simcyp Simulator including a first-order absorption model and the advanced dissolution absorption metabolism (ADAM) model (Jamei *et al.,* 2009).

Prediction of first order absorption (fa) and associated rate constant (ka)

For the fraction absorbed (fa) and first order absorption rate constant (ka), *in vivo* values and associated variability can be used as inputs. Alternatively, Equation 2 and Equation 3 can be used to predict fa and ka from an estimate of *in vivo* permeability, $P_{eff,man}$, (Yu *et al*., 1998). Several methods can be used within the Simcyp Simulator to predict $P_{eff,man}$ for a given drug. These are based on apparent permeability data obtained with cell lines (Caco-2, MDCK, LLC-PK1) (Sun *et al.,* 2002, Tchaparian *et al*., 2008), the PAMPA system or QSAR based on physicochemical properties (PSA and HBD, Winiwarter *et al.,* 1998).

$$ka = \frac{2 \times P_{eff,man}}{R}$$

Equation (1)

$$fa = 1 - (1 + 0.54\ P_{eff,man})^{-7}$$

Equation (2)

Prediction of Clearance

Clearance (CL) can be predicted from either human liver microsome (HLM) data or from human hepatocyte (HHep) data using Equation 4 and Equation 5.

$$CLu_{\text{int}H-pe} = \frac{CL_{\text{int}-pe}}{fu_{mic-pe}} \times Uptake \times MPPGL \times LiverWt \times 60 \times 10^{-6}$$

(Equation 4)

$$CLu_{\text{int}H-pe} = \frac{CL_{\text{int}-pe}}{fu_{inc-pe}} \times Uptake \times HPGL \times LiverWt \times 60 \times 10^{-6}$$

(Equation 5)

Where $CL_{intH\text{-}pe}$ is the CL in HLM by pathway 'p' by enzyme 'e' per mg microsomal protein, or CL in HHep by pathway 'p' by enzyme 'e' per million cells, MPPGL is the amount (mg) of microsomal protein per gram of liver, HPGL is the total number (in million) of hepatocytes per gram of liver, fu_{mic} is the free fraction of drug in the microsomal incubation, fu_{inc} is the free fraction of drug in the hepatocyte incubation, 'Uptake' is a factor that accounts for any active hepatic uptake (default value = 1) and 'LiverWt' is the liver weight of an individual, '60 x 10^{-6}' is a unit conversion factor.

Hence, total unbound intrinsic hepatic clearance ($CLu_{int,H\text{-}pe}$) is given by the sum of all intrinsic clearances by all enzymes and pathways (Equation 6).

$$CLu_{\text{int},H} = \sum_{p=1}^{n}\sum_{e=1}^{m} CLu_{\text{int},H-pe}$$

(Equation 6)

Where n is the number of pathways and m is the number of enzymes involved in the metabolism of the substrate. This intrinsic clearance value is applied in association with a prediction of drug distribution and through a number of differential equations (PBPK model) to generate a plasma drug concentration-time profile.

Prediction of First Pass Metabolism in the Gut (F_G)

To estimate intestinal availability (F_G), a model of 'first pass' metabolism, similar to the 'well-stirred liver', (Rostami-Hodjegan and Tucker, 2004) is used for substrates metabolised primarily by CYP3A but also by CYP2D6, CYP2C9 and CYP2C19 (Equation 7). In contrast to the 'well-stirred' liver model, the flow term (Q_{gut}) represents a nominal blood flow and is a hybrid parameter reflecting drug absorption rate from the gut lumen, removal of drug from the

enterocyte by the enterocytic blood supply and the volume of enterocytes. The free fraction of drug within the enterocyte is represented by the fu_{gut} term.

$$F_G = \frac{Q_{gut}}{Q_{gut} + fu_{gut} \times CL_{uG,int}}$$

(Equation 7)

The Q_{gut} term can be expanded in terms of its fundamental parameters:

$$Q_{gut} = \frac{Q_{villi} \text{ x } CL_{perm}}{Q_{villi} + CL_{perm}}$$

(Equation 8)

Where Q_{villi} is the villous blood flow (6% of the cardiac output in the Simulator) and CL_{perm} is a clearance term defining the permeability through the enterocyte.

$$CL_{perm} = P_{eff,man} \text{ x } A$$

(Equation 9)

CL_{perm} is the product of the value for effective intestinal permeability in man ($P_{eff,man}$) and A is the net cylindrical surface area of the small intestine (Yang *et al*., 2007).

In the absence of any information on active drug uptake into the enterocyte, fu_{gut} is set at a default value of 1 (which assumes that there is insufficient time for plasma protein binding equilibrium or erythrocyte uptake before the drug is removed from the basolateral side of the enterocyte). However, it may also be set at fu_p which assumes that there is sufficient time for plasma protein binding equilibrium. Assuming that a proportional relationship exists between Q_{gut} and permeability (P_{app}) data obtained using Caco-2 cells, a Q_{gut} value can be estimated (Yang *et al.,* 2007). For calculation of gut intrinsic clearance ($CLu_{G,int}$), the CYP3A-mediated hepatic CLu_{int} is divided by the abundance of CYP3A in liver (137 pmol P450/mg protein) to obtain the CLu_{int} in terms of µl/min per pmol P450. Using a mean abundance of 70000 pmol CYP3A/total gut this value is scaled to a whole gut CLu_{int} value (Yang *et al*., 2004). The assumption that the intrinsic clearance per pmol CYP is the same in both gut and liver is supported by observations on a number of drugs, such that hepatic rather than intestinal microsomal data can be used (Yang *et al*., 2004).

Prediction of F_H and F

The 'well-stirred' model of hepatic clearance was used to estimate the fraction avoiding first-pass metabolism in the liver (F_H).

$$F_H = \frac{Q_H}{Q_H + fu_B \times CLu_{H.int}}$$

(Equation 10)

where Q_H (hepatic blood flow), fu_B (the fraction of drug unbound in blood) and $CLu_{H,int}$ (intrinsic metabolic clearance) are the primary determinants of net hepatic clearance (CL_H). Thus, following oral administration, bioavailability F can be estimated using Equation 11:

$$F = fa.F_G.F_H$$

(Equation 11)

Enzyme Dynamics and Inhibition

Changes in metabolic clearance due to reversible inhibition of enzyme activity, or changes in enzyme levels due to mechanism-based inactivation and/or induction can be handled using mechanistic dynamic models within the Simcyp Simulator. The underlying assumptions and operating differential equations have been described in detail elsewhere (Rowland Yeo *et al*., 2010; Rowland Yeo *et al*., 2011). Unbound concentrations of inhibitor in the liver and portal vein are used as the driving force for inhibition of metabolism in the liver and gut, respectively. Values of the intrinsic turnover of hepatic and gut CYP3A4 (k_{deg}) used in the simulations involving induction of CYP3A4 by rifampicin were 0.019 h^{-1} and 0.03 h^{-1}, respectively (Rowland Yeo *et al.,* 2011; Yang *et al*., 2008).

References

1. Berezhkovskiy LM (2004) Volume of distribution at steady state for a linear pharmacokinetic system with peripheral elimination. *J Pharm Sci* **93:**1628-1640.
2. Gaohua L, Turner DB, Fisher C, Emami Riedmaier A, Musther H, Gardner I and Jamei M A novel mechanistic approach to predict the steady state volume of distribution (Vss) using the Fick-Nernst-Planck equation [abstract], in: PAGE. Abstracts of the Annual Meeting of the Population Approach Group in Europe June 2016; Lisbon, Portugal. Abstr 5709.
3. Jamei M, Turner D, Yang J *et al.* Population-based mechanistic prediction of oral drug absorption. *AAPS J* 2009; 11, 225-237.
4. Poulin P and Theil FP. Prediction of pharmacokinetics prior to in vivo studies 1. Mechanism-based prediction of volume of distribution. *J Pharm Sci* 2002; 91:129-156.
5. Rodgers T and Rowland M. Physiologically based pharmacokinetic modelling 2: predicting the tissue distribution of acids, very weak bases, neutrals and zwitterions. J Pharm Sci. 2006; 95(6):1238-57.

6. Rostami-Hodjegan A and Tucker GT. *'In silico'* simulations to assess the 'in vivo' consequences of *'in vitro'* metabolic drug-drug interactions. *Drug Discov Today: Technology* 2004;1(4):441-8.

7. Rowland-Yeo K, Jamei M, Yang J, Tucker GT and Rostami-Hodjegan A. Physiologically based mechanistic modelling to predict complex drug–drug interactions involving simultaneous competitive and time-dependent enzyme inhibition by parent compound and its metabolite in both liver and gut - the effect of diltiazem on the time-course of exposure to triazolam. *Eur J Pharm Sci* 2010; 39:298-309.

8. Rowland Yeo K, Walsky RL, Jamei M, Rostami-Hodjegan A and Tucker GT (2011) Prediction of time-dependent CYP3A4 drug-drug interactions by physiologically based pharmacokinetic modelling: impact of inactivation parameters and enzyme turnover. *Eur J Pharm Sci* **43:**160-173.

9. Sawada Y, Hanano M, Sugiyama Y, Harashima H and Iga T. Prediction of the volumes of distribution of basic drugs in humans based on data from animals. *J Pharmacokinet Biopharm* 1984; 12:587-596.

10. Sun D, Lennernas H, Welage LS, Barnett JL, Landowski CP, Foster D, Fleisher D, Lee KD and Amidon GL. Comparison of human duodenum and Caco-2 gene expression profiles for 12,000 gene sequences tags and correlation with permeability of 26 drugs. Pharmacol Res 2002; 19: 1400-06.

11. Tchaparian E, Tang L, Xu G, Huang T and Jin L Cell based experimental models as tools for the prediction of human intestinal absorption [abstract], in: ISSX Online Abstracts Supplement 3 (3); October 2008; San Diego, CA. Abstr 245.

12. Winiwarter S, Bonham NM, Ax F, Hallberg A, Lennernas H and Karlen A Correlation of human jejunal permeability (in vivo) of drugs with experimentally and theoretically derived parameters. A multivariate data analysis approach. J Med Chem 1998; 41:4939-4949.

13. Yang J, Tucker GT and Rostami-Hodjegan A. Cytochrome P450 3A expression and activity in the human small intestine. Clin Pharmacol Ther 2004; 76: 391.

14. Yang J, Jamei M, Rowland-Yeo K, Tucker GT and Rostami-Hodjegan A. Prediction of intestinal first-pass metabolism. *Curr Drug Metab* 8: 676-684 (2007).

15. Yang J, Liao M, Shou M, Jamei M, Rowland-Yeo K, Tucker GT and Rostami-Hodjegan A. Cytochrome P450 turnover: regulation of synthesis and degradation, methods for determining rates, and implications for the prediction of drug interactions. *Curr Drug Metab* 2008; 9: 384-394 (2008).

16. Yu LX and Amidon GL. Saturable small intestine drug absorption in humans: modelling and interpretation of cefatrizine data. Eur J Pharm Biopharm 1998; 45: 199-203.